

# Polarized quantum dot emission from photonic crystal nanocavities studied under mode-resonant enhanced excitation

R. Oulton<sup>1\*</sup>, B.D. Jones<sup>1</sup>, S. Lam<sup>1</sup>, A.R.A. Chalcraft<sup>1</sup>, D. Szymanski<sup>1,2</sup>, D. O'Brien<sup>2</sup>, T.F. Krauss<sup>2</sup>, D. Sanvitto<sup>3</sup>, A.M. Fox<sup>1</sup>, D.M. Whittaker<sup>1</sup>, M. Hopkinson<sup>4</sup>, M.S. Skolnick<sup>1</sup>,

<sup>1</sup>*Dept. of Physics and Astronomy, University of Sheffield, Hicks Building, Hounsfield Rd., Sheffield, S3 7RH, UK*

<sup>2</sup>*School of Physics and Astronomy, The University of St. Andrews, KY16 9SS, UK*

<sup>3</sup>*Universidad Autonoma, Depto. Fisica de Materiales C - IV, 612, C/ Francisco Tomás y Valiente n° 7, Cantoblanco, 28049 Madrid, SPAIN*

<sup>4</sup>*EPSRC National Centre for III-V Technologies, Dept. of Electrical and Electronic Engineering, University of Sheffield, Sheffield S1 3JD, UK*

\*Corresponding author: [R.Oulton@Sheffield.ac.uk](mailto:R.Oulton@Sheffield.ac.uk)

**Abstract:** We study the linear polarization of the emission from single quantum dots embedded in an “L3” defect nanocavity in a two-dimensional photonic crystal. By using narrow linewidth optical excitation in resonance with higher-order modes, we are able to achieve strong quantum dot emission intensity whilst reducing the background from quantum dots in the surrounding lattice. We find that all the dots observed emit very strongly linearly polarized light of the same orientation as the closest mode, despite the fact that these quantum dots may be spectrally detuned by several times the mode linewidth. We discuss the coupling mechanisms which may explain this behavior.

©2007 Optical Society of America

OCIS codes: (230.5298) Photonic crystals, (230.5590) Quantum-well, -wire and -dot devices.

---

## References and links

1. K.J. Vahala, “Optical Microcavities,” *Nature* **424**, 839-846 (2003) and references therein
2. T. Yoshie, A. Scherer, J. Hendrickson, G. Khitrova, H. M. Gibbs, G. Rupper, C. Ell, O. B. Shchekin and D. G. Deppe, “Vacuum Rabi splitting with a single quantum dot in a photonic crystal nanocavity,” *Nature* **432**, 200-203 (2004)
3. J. P. Reithmaier, G. Sek, A. Löffler, C. Hofmann, S. Kuhn, S. Reitzenstein, L. V. Keldysh, V. D. Kulakovskii, T. L. Reinecke and A. Forchel, “Strong coupling in a single quantum dot–semiconductor microcavity system,” *Nature* **432**, 197-200 (2004)
4. E. Peter, P. Senellart, D. Martrou, A. Lemaître, J. Hours, J. M. Gérard, and J. Bloch, “Exciton-Photon Strong-Coupling Regime for a Single Quantum Dot Embedded in a Microcavity,” *Phys. Rev. Lett* **95** 067401-067404 (2005)
5. Y. Tanaka, J. Upham, T. Nagashima, T. Sugiya, T. Asano, S. Noda, “Dynamic Control of the Q-factor in a Photonic Crystal Nanocavity,” *Nature Materials* **6**, 862-865 (2007)
6. Y. Akahane, T. Asano, B.-S. Song, S. Noda, “High-Q nanocavity in a two-dimensional photonic crystal,” *Nature* **425**, 944-947 (2003)
7. A. Faraon, D. Englund, I. Fushman, J. Vučković, “Local Quantum Dot Tuning on Photonic Crystal Chips,” *Appl. Phys. Lett.* **90**, 213110-213113 (2007)
8. K. Hennessy, A. Badolato, M. Winger, D. Gerace, M. Atatüre, S. Gulde, S. Fält, E.L. Hu, A. Imamoglu “Quantum nature of a strongly coupled single quantum dot–cavity system,” *Nature* **445**, 896-899 (2007)
9. A. Chalcraft, S. Lam, D O'Brien, T.F. Krauss, M. Sahin, D. Szymanski, D. Sanvitto, R. Oulton, M. S. Skolnick, A. M. Fox, D. M. Whittaker, H.-Y. Liu and M. Hopkinson, “Mode structure of the L3 photonic crystal cavity,” *Appl. Phys. Lett.* **90**, 241117-241119 (2007)
10. D. Press, S. Götzinger, S. Reitzenstein, C. Hofmann, A. Löffler, M. Kamp, A. Forchel, Y. Yamamoto, “Photon antibunching from a single quantum-dot-microcavity system in the strong coupling regime,” *Phys. Rev. Lett* **98**, 117402-117405 (2007)
11. M. Kaniber, A. Kress, A. Laucht, M. Bichler, R. Meyer, M.-C. Amann and J.J. Finley, “Efficient spatial redistribution of quantum dot spontaneous emission from two-dimensional photonic crystals,” *Appl. Phys. Lett.* **91**, 061106-061108 (2007)

12. M. Nomura, S. Iwamoto, T. Nakaoka, S. Ishida and Y. Arakawa, "Localised excitation of InGaAs quantum dots by utilizing a photonic crystal nanocavity," *Appl. Phys. Lett.* **88**, 141108-141110 (2006)
  13. M. Nomura, S. Iwamoto, T. Nakaoka, S. Ishida and Y. Arakawa, "Cavity resonant excitation of InGaAs quantum dots in photonic crystal nanocavities," *Jpn. J. Appl. Phys.* **45**, 6091-6095 (2006)
  14. W.C. Stumpf, M. Fujita, M. Yamaguchi, T. Asano, S. Noda, "Light-emission properties of quantum dots embedded in a photonic double-heterostructure nanocavity," *Appl. Phys. Lett.* **90**, 231101-231103 (2007)
  15. D.M. Whittaker, I.S. Culshaw, V.N. Astratov, M.S. Skolnick, "Photonic bandstructure of patterned waveguides with dielectric and metallic cladding," *Phys. Rev. B* **65** 073102-073105 (2002)
  16. L.C. Andreani, D. Gerace, "Photonic-crystal slabs with a triangular lattice of triangular holes investigated using a guided-mode expansion method," *Phys. Rev. B* **73**, 235114-235130 (2006)
  17. M. Nomura, S. Iwamoto, T. Yang, S. Ishida and Y. Arakawa, "Enhancement of light emission from single quantum dot in photonic crystal nanocavity by using cavity resonant excitation," *Appl. Phys Lett* **89**, 241124-241126 (2006)
  18. A. Vasanelli, R. Ferreira, and G. Bastard, "Continuous Absorption Background and Decoherence in Quantum Dots," *Phys. Rev. Lett.* **89**, 216804-216807 (2002)
  19. R. Oulton, J.J. Finley, A. Tartakovskii, D.J. Mowbray, M.S. Skolnick, M. Hopkinson, A. Vasanelli, R. Ferreira and G. Bastard, "Continuum transitions and phonon coupling in single self-assembled Stranski-Krastanow quantum dots," *Phys. Rev. B* **68**, 235301-235304 (2003)
  20. M. Bayer, G. Ortner, O. Stern, A. Kuther, A.A. Gorbunov, A. Forchel, P. Hawrylak, S. Fafard, K. Hinzer, T.L. Reinecke, S.N. Walck, J.P. Reithmaier, F. Klopff and F. Schäfer, "Fine Structure of neutral and charged excitons in self-assembled In(Ga)As/(Al)GaAs quantum dots," *Phys. Rev. B* **65**, 195315-195338 (2002)
  21. A. Daraei, D. Sanvitto, J.A. Timpson, A.M. Fox, D.M. Whittaker, M.S. Skolnick, P.S.S. Guimarães, H. Vinck, A. Tahraoui, P.W. Fry, S.L. Liew and M. Hopkinson, "Control of polarization and mode mapping of small volume high Q micropillars," *J. Appl. Phys.* **102**, 043105-043110 (2007)
  22. J.A. Timpson, D. Sanvitto, A. Daraei, P.S.S. Guimarães, A. Tahraoui, P.W. Fry, M. Hopkinson, D.M. Whittaker, A.M. Fox, M.S. Skolnick, "Polarization control and emission enhancement of a quantum dot in ultra-high finesse microcavity pillars," *Physica E* **32**, 500-503 (2006)
  23. M. Bayer, T. L. Reinecke, F. Weidner, A. Larionov, A. McDonald, and A. Forchel "Inhibition and Enhancement of the Spontaneous Emission of Quantum Dots in Structured Microresonators," *Phys. Rev. Lett.* **86**, 3168-3171 (2001)
  24. A. Kress, F. Hofbauer, N. Reinelt, M. Kaniber, H.J. Krenner, R. Meyer, G. Böhm and J.J. Finley "Manipulation of the spontaneous emission dynamics of quantum dots in two-dimensional photonic crystals," *Phys. Rev. B* **71**, 241304(R)-241307 (2005)
- 

## 1. Introduction

Of the many proposals for the implementation of quantum information schemes, those involving semiconductor quantum dots (QDs) embedded in a photonic structure have received a great deal of attention [1], as they hold the promise of bridging the gap between atomic cavity quantum electrodynamics and solid-state semiconductor devices. Particular attention is being paid to increasing and controlling the interaction of the QD with photons. By embedding QDs into micropillars, microdisk resonators or photonic crystal nanocavities, the light-matter interaction strength has been shown to increase to the point of strong coupling [2-4]. One type of photonic cavity structure, the photonic crystal (PhC) nanocavity, holds a great deal of promise, not only due to the very high quality factors and ultra-low modal volumes achievable, but also because flexibility in cavity geometry is inherent in the choice of cavity design. Many cavity designs have been demonstrated, along with more complicated structures including coupled cavities and cavities coupled to 2-D waveguides [5]. This is the point at which QD-cavity QED begins to extend beyond that which is possible in atomic systems.

In this Article we present work on a particular type of PhC cavity, namely an "L3" defect cavity [6], which has attracted a great deal of attention as the only PhC cavity in which strong coupling with a QD exciton has been observed [2,7,8]. In a previous publication, we investigated the properties of the higher order modes that may be supported in these cavities [9]. We demonstrate here that by exciting resonantly at the wavelength of these higher-order modes, efficient optical excitation of both the fundamental cavity mode and individual QDs inside the cavity may be achieved, whilst dramatically reducing background emission from QDs outside of the cavity region. We also investigate the polarization of single QD emission observed when exciting on-resonance with the higher-order modes. Our previous work revealed that the emission of all of the L3 cavity modes is strongly polarized [9]. Here we

demonstrate that all of the single QD features we observe are strongly polarized in the same direction as the closest mode, despite the fact that the QDs themselves may be detuned by as many as sixteen times the mode linewidth. Such results not only suggest that the excitation conditions result in only QDs inside the cavity region being excited, but that a mechanism exists that allows coupling of the QD transitions to a mode even when far from resonance. These results are in agreement with a recent report demonstrating off-resonant exciton-mode anticorrelation in a dot-cavity system where strong coupling is observed on resonance [8,10].

## 2. Nanocavity excitation using higher-order mode excitation

The samples studied were fabricated from a wafer grown by molecular beam epitaxy containing a 140nm thick GaAs membrane into which a single layer of InGaAs QDs at a density of  $\sim 10^{10}\text{cm}^{-2}$  was incorporated. Fig 1(a) shows the photoluminescence (PL) spectrum of the unpatterned wafer (grey spectrum), revealing QD ensemble emission at 4K centred at  $\sim 910\text{nm}$  with a FWHM of  $\sim 40\text{nm}$ . The wafer was processed into hexagonal lattice PhC structures of circular air holes using electron beam lithography and chemically-assisted ion beam etching. A range of lattice constants  $230 \leq a \leq 290\text{nm}$ , and fill-factors  $0.25 \leq r/a \leq 0.33$  was produced to provide a wide range of fundamental and higher order modes. "L3" defects are incorporated into the lattice, consisting of a line of three holes missing along the  $\Gamma$ -K ("x") direction of the lattice. The two end holes were displaced along  $x$  by a factor  $s = 0.15a$  as described in Ref.[9].

As reported previously for similarly designed structures [9], several modes may be supported in the cavity. Cavity emission is investigated using a standard micro-PL set-up as described in Ref [9]. Fig 1(a) (red and blue spectra) shows the linearly polarization resolved PL emission of a particular example, Cavity A, with lattice constant  $a = 275\text{nm}$ , using non-resonant illumination at  $633\text{nm}$ . High intensity excitation is used such that the mode emission dominates over any individual QD features.

The QD ensemble emission region covers five optical modes, with all showing a strong linear polarization. Fig 1(b) shows polar plots of the mode intensity vs linear polarization for modes 1-3,5. The fundamental mode (M1) at  $994\text{nm}$  has the highest Q-value of  $\lambda/\Delta\lambda \sim 5400$ . Its polarization is  $\rho = 55\%$ , defined as  $\rho = (I_{\max} - I_{\min}) / (I_{\max} + I_{\min})$ , where  $I_{\max}$  and  $I_{\min}$  are the intensities at the maximum and minimum of the polar plot. The polarization axis is found to lie at  $\sim 70^\circ$  to the  $x$ -direction. Further lower-Q value modes are observed to shorter wavelength, and are denoted M2 ( $\rho = 49\%$  polarized along the  $y$ -direction, with  $Q \sim 1500$ ), M3 ( $\rho = 87\%$  polarized along  $x$  with Q-value 1200), M4 (also polarized along  $x$ , but due to the high density of QD features, the polarization magnitude and Q is difficult to determine) and M5 ( $\rho = 88\%$  polarized along  $y$ , Q-value  $\sim 1000$ ). The polarization of these modes is discussed in detail in Ref [9].

The design of this L3 cavity, with shifted end-holes, is optimized to maximize the Q-value of the fundamental mode wavelength, by suppressing the coupling of light inside the cavity to the outside environment. However, the higher-order modes are far leakier, as indicated by the lower Q-values. As emission in the in-plane direction is expected to be strongly suppressed due to the photonic crystal lattice [11], light emitted into the higher-order cavity mode couples preferentially to the out-of-plane directions.

The fact that the higher-order modes are "leaky" in the vertical direction may be used to our advantage. It has been shown in both L3 [12,13] and double-heterostructure type [14] cavities that resonantly exciting at the wavelength of one of the higher-order modes using a narrow ( $\sim 20\mu\text{eV}$ ) linewidth laser results in strong light absorption, and subsequent intense emission from lower-order modes, as well as suppression of background emission. We can explain this observation by reference to the calculated cavity mode patterns. Fig 1(c) shows the calculated  $|E|^2$  intensity patterns for Modes 1-3 and 5, calculated using the guided-mode expansion method as in ref [9,15,16], in the centre of the membrane for a structure with lattice constant  $a = 275\text{nm}$ , hole radius ratio  $r/a = 0.31$  and end-hole shift  $s = 0.15a$ . The calculated spectral position, relative intensity and polarization of the modes were found to agree well

with the experimental data. Mode 4 is not shown – in fact calculations show that this is likely to consist of two spectrally close, low Q modes. The polarization of both of these modes is however predominantly along  $x$ .

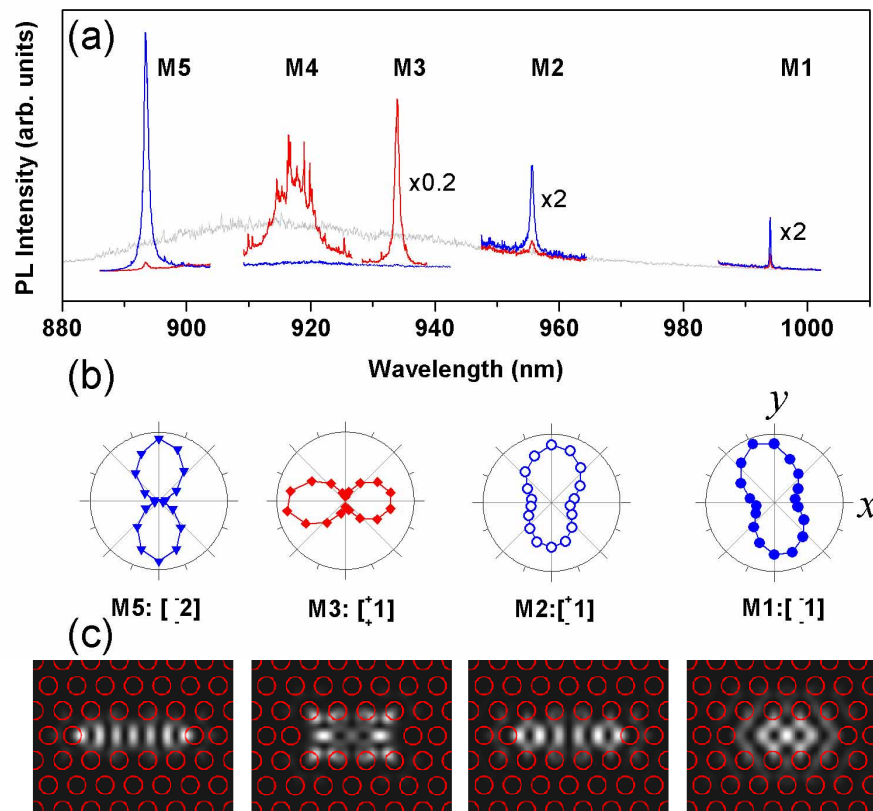


Fig. 1. (a) Photoluminescence spectra of Cavity A taken at high excitation power with non-resonant excitation, detecting linear polarization along  $x$  (red) and along  $y$  (blue) to the  $\Gamma$ -K photonic lattice axis. The grey spectrum shows the ensemble QD PL emission on an unpatterned part of the wafer. (b) Polar PL intensity plots of modes M1- M3, M5.  $x$  ( $y$ ) corresponds to  $0^\circ$  ( $90^\circ$ ) relative to the defect axis. Modes are labelled according to their parity along the  $x$  (upper labels) and  $y$  axes (lower labels), as described in ref [9]. (c)  $|E|^2$  mode patterns for modes 1-3 and 5 for Cavity A calculated using the guided-mode expansion method [9,15,16].

Whilst the intensity patterns vary between modes, it is clear that the electric field is concentrated within the cavity region in all cases. Light impinging on the structure and resonant with one of the higher-order modes will couple much more strongly to the areas in the cavity where the electric field is non-zero. The light persists in the cavity longer, such that the absorption probability increases. Carriers are subsequently excited and relax in energy to the QD ground states, where they are observed in PL emission. Carriers are selectively excited inside the cavity, and relaxation into the QD ground states is fast enough that carrier diffusion throughout the device is highly unlikely to occur. This means that only QDs inside the cavity region will be excited. This has a great advantage over optically exciting at energies above the photonic band gap. In the latter case, absorption occurs with uniform probability across the illuminated region. The spatial resolution is therefore governed by the resolution of the microscope objective (in our case about  $2\mu\text{m}$ ), which is much larger than the cavity. In this case, QDs in the entire illuminated region are excited such that the desired

emission from a QD inside the cavity may be obscured by background QD emission in the surrounding lattice.

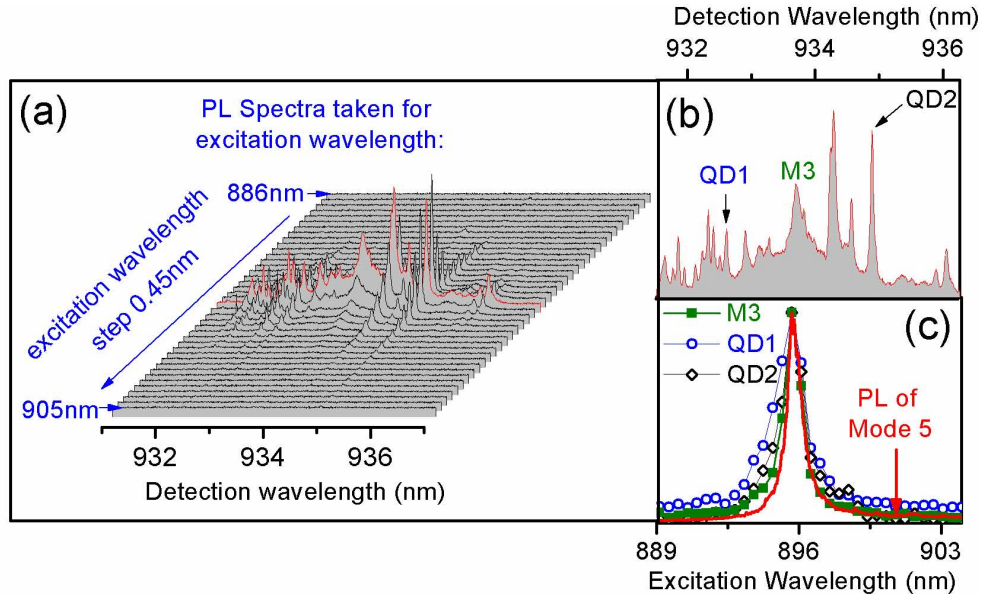


Fig. 2. (a) Multichannel photoluminescence excitation (PLE) spectra of Cavity A. The excitation power is kept such that both the mode and several QD features are observed, and the wavelength of the exciting laser stepped from 886nm (below the wavelength of Mode 5) to 905nm (above the wavelength of Mode 5). A spectrum is taken at each step. The spectra are shifted both vertically and horizontally for clarity. (b) Spectrum around Mode 3 taken for the excitation wavelength which gives maximum intensity (indicated in red in (a)). (c) Normalized intensity of Mode 3 (green squares), QD 1 (blue open circles), QD 2 (black open diamonds) as a function of excitation wavelength (PLE spectra). The spectral positions of these features are shown in (b). The PL of Mode 5 (red) taken from Fig 1(a) is also shown for comparison.

In Fig 2 we demonstrate the operation of this technique in one of our devices, Cavity A. Here the effect of exciting with a  $20\mu\text{eV}$  linewidth CW Ti:Sapphire laser resonant with Mode 5 [see Fig 1(a)] is demonstrated by observing the PL emission around Mode 3. The laser is tuned from below the Mode 5 wavelength at 886nm to above it at 905nm in 0.45nm steps, with a CCD spectrum taken at each wavelength. The excitation polarization was matched to that of Mode 5, and the excitation intensity adjusted such that both the background emission from Mode 3 and single QD features were observed. The resulting multichannel photoluminescence excitation (PLE) spectrum is shown in Fig 2(a). Off-resonance with Mode 5, very little emission is observed, but as the laser is tuned into resonance, several PL features appear which increase in intensity until the laser is exactly on resonance with Mode 5. Fig 2(b) shows the PL spectrum taken when the laser is on resonance. A broad background arises from the Mode 3 emission and peaks at the point marked M3. Superimposed onto the mode emission are several sharp features that correspond to emission from single QDs. Careful measurement of the intensity of features M3, QD1 and QD2 reveals that the intensity ratio of on-resonant to off-resonant excitation is  $\sim 90:1$  or greater. In fact no PL emission above that of the background noise could be observed off-resonance at  $\lambda_{\text{ex}} = 905\text{nm}$ .

To verify that the intensity of the emission does indeed correspond directly to resonant absorption into Mode 5, Fig 2(c) shows a plot of the normalized intensity as a function of excitation wavelength of feature M3 (green squares), as well as two single QD features (blue and black open circles) labelled in Fig 2(b). Also shown is a normalized PL spectrum of Mode 5 taken with non-resonant excitation. All three PLE spectra closely follow the intensity

profile of the PL spectrum of Mode 5, indicating that their absorption spectra are almost entirely governed by the wavelength-dependent local light enhancement into Mode 5.

The fact that the absorption density of states is close to uniform over the measured range might appear surprising, since for single QDs, one might expect to observe absorption only when on resonance with a sharp excited state (as observed using similar techniques in Ref [17]). We therefore speculate that a continuum of absorption states exists for these QDs, as described in Refs [18,19]. Electron-hole pairs may be created via crossed transitions, where one carrier is absorbed into the wetting layer, and the other into the QD ground state. Subsequent energy relaxation results in both carriers occupying the ground state. As the transitions involve the wetting layer, the absorption density of states not only consists of sharp “p-shell” states but also a smooth continuum of available transitions. If this is the case, all QDs with ground states below the excitation energy would be excited as long as they have the correct spatial position (i.e. inside the cavity). Thus this resonant cavity-enhanced excitation technique would appear to be an efficient and simple way to excite selectively all QDs inside the cavity which couple to the modes.

### 3. Determination of QD-mode coupling from strongly polarized emission

Let us now consider the polarization of the single QD emission. In Fig 1, it was demonstrated that each of the modes is strongly polarized due to the symmetries of the cavity and underlying PhC lattice. In Ref [14] it was shown for a double heterostructure cavity that light could only be resonantly coupled into the cavity mode if the excitation laser was co-polarized to the higher-order mode. We tested this assertion for our case: again, the laser was resonantly tuned to Mode 5, and the PL intensity from Mode 3 monitored. Fig 3(a) shows two spectra taken of Mode 3, with excitation polarization along  $y$  (co-polarized to Mode 5) and along  $x$  (cross-polarized to Mode 5). In this case the excitation intensity was increased such that only emission from the mode is observed. The detection polarization was co-polarized to Mode 3 along  $x$ . Similarly to Ref [14], under cross-polarized excitation almost no emission is observed at Mode 3, with the intensity ratio  $I(\text{co}):I(\text{cross}) > 200:1$ .

We now turn our attention to the polarization of the emission around the Mode 3 region. As before, the excitation was tuned to Mode 5 with the excitation polarization along  $y$ , co-polarized to Mode 5. The excitation intensity was reduced to allow observation of single QD features. Fig 3(b) shows PL spectra for the region around Mode 3, with polarization detection along  $x$  (co-polarized to Mode 3) and  $y$  (cross-polarized to Mode 3, but co-polarized to Mode 5). As expected, the broad background emission from the mode, centered at 933nm, is strongly polarized. However, several sharp features that correspond to single QD transitions are also observable, both on-resonance and several nm away from Mode 3. Again, all of these transitions are strongly polarized. The polarization of each QD line is indicated in Fig 3(c), where positive polarization indicates polarization at  $0^\circ$  along the  $x$ -axis. All of the QD features have polarization  $\rho > 70\%$ . These results are rather surprising, as strongly polarized QD emission is typically only observed when carriers retain their spin orientation from the excitation. This is not the case here, where the excitation is along  $y$  and the detection polarization along  $x$ . Linearly polarized doublets may be observed in high resolution experiments [20], but both orthogonal polarizations should be observed in the case where the fine structure splitting is greater than the spectral resolution. One should therefore not expect to observe strongly polarized QD emission in the orthogonal direction to the excitation polarization.

One possible explanation is that the polarization of the QD emission is strongly influenced by the presence of the optical cavity mode. Such effects have already been observed in QD elliptical micropillar devices [21,22]. In this case a QD on resonance with a polarized mode experiences Purcell enhancement and greatly enhanced light emission. Enhancement occurs, however, only for the QD polarization that matches that of the mode: the orthogonal QD polarization is not enhanced, and thus the QD polarization is strongly linearly co-polarized with the mode. We will demonstrate in the following two figures that the QD emission polarization is strongly co-polarized to the polarization of the closest cavity

mode regardless of whether they are polarized along  $x$  or  $y$ . This indicates that the mode fully governs the polarization of the QD emission. For example, even if the QDs display an intrinsic PL polarization due to asymmetry along a particular crystal direction, this would be independent of the cavity mode polarization. In fact, QD emission polarizations were measured in several different cavities and in all cases it was found that the QD emission was strongly influenced by the closest mode.

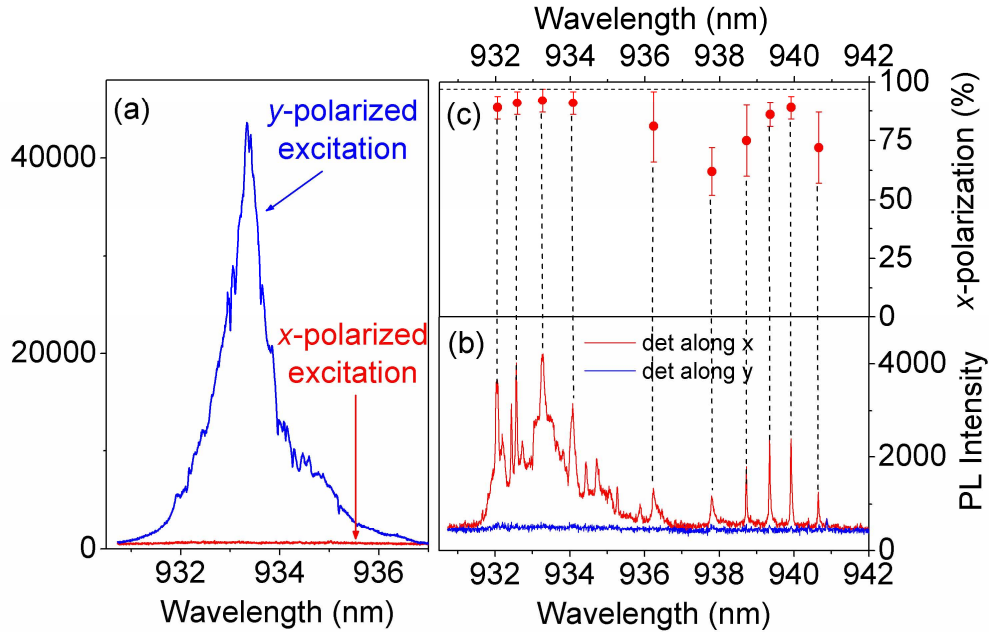


Fig. 3. (a) PL emission from Cavity A at Mode 3, taken for excitation with a CW Ti:sapphire laser tuned to be resonant with the wavelength of Mode 5. Blue shows excitation polarization co-linear with the polarization of Mode 5 (along  $y$ ), red for opposite linear polarization (along  $x$ ). The excitation power was chosen to be strong enough that the Mode 3 emission dominates over single QD features. The detection polarization was chosen to match that of Mode 3 (along  $x$ ). (b) PL spectrum around Mode 3 at lower excitation intensity, showing both QD and mode features. The excitation polarization was kept along  $y$ , with the detection polarization along  $y$  (blue) or along  $x$  (red). (c) Linear polarization, defined as  $\rho = [I(x)-I(y)]/[I(x)+I(y)]$  of single QD features from (b). The dashed line indicates the polarization of Mode 3 at high power.

Figure 3(b) shows several QD lines over the spectral range 931-935 nm superimposed on the Mode 3 emission. The lines are all strongly co-polarized ( $\rho > 90\%$ ) with Mode 3. Clearly, QD polarization is enhanced when on resonance with the mode. However, the behavior of QDs detuned from Mode 3 is also surprising: in the spectral region 938-941 nm four QD lines are observed that are also strongly co-polarized ( $\rho = 75-90\%$ ) to Mode 3. Given that these features are at least one mode linewidth away from Mode 3, one would expect a greatly reduced coupling to the mode, and almost no enhancement of the QD polarization. We contrast these results in particular to those found in elliptical micropillars [22], where it was found that a QD feature temperature-detuned to approximately one linewidth away from the mode showed  $\rho \sim 0$ . The elliptical micropillar, however, has two orthogonal modes separated from each other by just a few nm, such that the system is not strictly comparable to the PhC.

Note also that all of the QD lines show strong polarization, implying that every QD observed couples to the cavity mode. This may be for one of two reasons: either all of the QDs inside the cavity region overlap sufficiently with Mode 3 (which is possible due to the fact that both Modes 3 and 5 are strongly localised inside the cavity region) or the Purcell

factor is so large for the QDs on-resonance with Mode 3 that, given the excitation intensity, these features dominate over more weakly emitting QDs that are not spatially well-positioned.

In order to investigate the effect of a detuned mode on the QD polarization in more detail, QD emission close to the fundamental mode was chosen for study, as this mode has a greater Q-value. The spectral detuning relative to the width of the mode is therefore very large, even for QD lines only a few nm away. As the fundamental mode in Cavity A lies at 994nm, the probability of finding a QD inside the cavity at this long wavelength is very small. Therefore, a second Cavity B, with lattice constant  $a = 260\text{nm}$ , was studied. In this cavity the fundamental mode occurs at 948nm, which is closer to the QD ensemble distribution. Resonant excitation was performed into a higher-order mode occurring at 895nm, corresponding to Mode 3 for this structure. The excitation polarization was along  $x$ , matching the polarization of the mode.

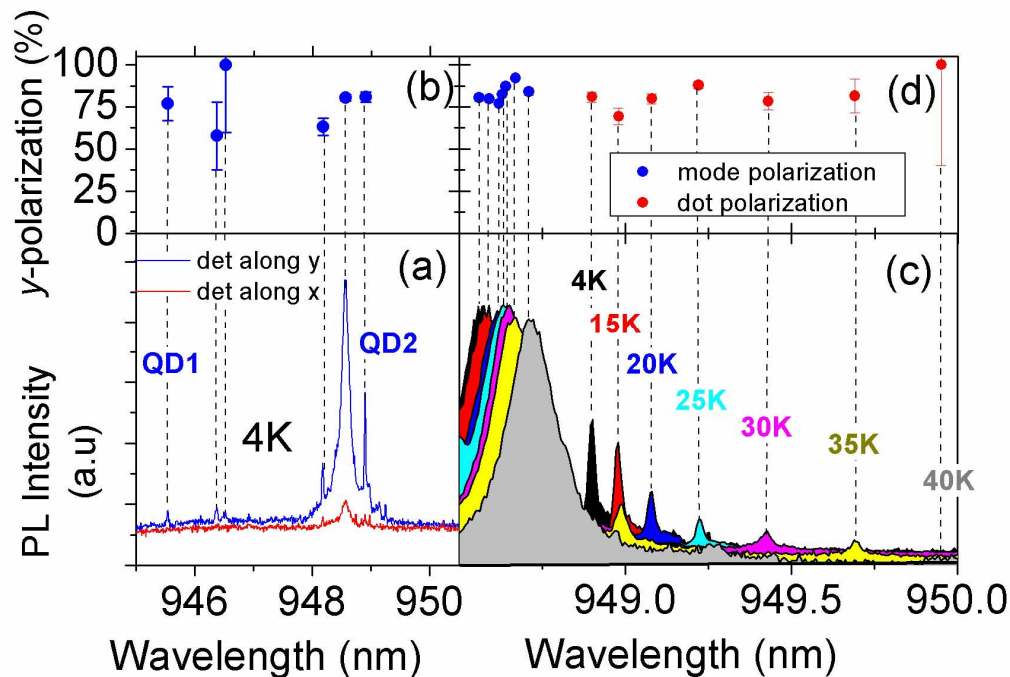


Fig. 4. (a) Photoluminescence spectra of Cavity B. The broad feature observed corresponds to the fundamental mode, and the sharp features to single QD lines. The PL is detected co-polarized ( $y$  - blue) and cross-polarized ( $x$  - red) to the mode. (b) Polarization of the mode and single QD lines observed over this spectral range. Positive polarization is along the  $y$ -direction. (c) PL spectra taken for increasing temperature, showing the mode and QD2 on the long wavelength side only. (d) Polarization of mode (blue) and QD (red) as a function of temperature.

Figure 4(a) shows PL spectra around the fundamental mode, taken along  $y$  (blue) and  $x$  (red). Again, the excitation intensity was adjusted such that both QD and mode emission were observed. The broad feature observed at 948.5nm corresponds to the fundamental mode, with a Q-value of  $\sim 5300$  and linewidth of  $\Delta\lambda = 0.18\text{nm}$ . The QDs lines that are just a few nm away are detuned by several mode linewidths. The QDs far from resonance from the mode have weak emission, while those on resonance have stronger emission. As in Fig 3(c), Fig 4(b) shows the polarization of both the mode and the QD lines, with positive polarization this time indicating polarization along  $y$ , co-polarized to the fundamental mode. While the fundamental mode is not as strongly polarized as the higher order modes ( $\rho_{\text{fund}} = 80\%$ ), one observes a strong polarization of all the QDs,  $58\% < \rho < 100\%$ , over a spectra range 946-950nm. Let us

take for example the weak line at 945.5nm (QD1), which has a polarization of  $\rho = 76\%$ . It would appear that the polarization of this QD is strongly influenced by the fundamental mode, despite the fact that it is detuned from the mode by 3nm, i.e. over  $16 \Delta\lambda$ . Note that the QD emission is now strongly y-polarized, compared to the QDs in Fig. 3, which are all strongly x-polarized, thus demonstrating that the strong QD polarization is determined by the mode polarization, and not intrinsic QD properties or the excitation polarization.

For such large detuning one might expect that Purcell enhancements of emission rate would be negligibly small. The spontaneous emission rate,  $1/\tau$ , of the QD transition compared to free-space,  $1/\tau_0$ , is given by[23]:

$$\frac{\tau_0}{\tau} = \frac{2}{3} F_p \frac{|\mathcal{E}(r)|^2}{|\mathcal{E}_{\max}|^2} \frac{\Delta\lambda^2}{\Delta\lambda^2 + 4(\lambda_c - \lambda_{QD})^2} + \alpha \quad (1)$$

where the first term describes the emission rate into the cavity mode:  $F_p$  gives the maximum Purcell factor on resonance,  $\mathcal{E}(r)$  the electric field distribution of the mode at position  $r$ , with  $\mathcal{E}_{\max}$  its maximum amplitude,  $\Delta\lambda$  is the linewidth of the mode,  $\lambda_c$  and  $\lambda_{QD}$  are the spectral positions of the mode and QD, respectively. For a detuning of  $16\Delta\lambda$  the Purcell enhancement should therefore be  $\sim 10^{-3}$  times the value on resonance. The second term,  $\alpha$ , gives the relative spontaneous emission rate into leaky modes.

The maximum Purcell factor is given by

$$F_p = \frac{3}{4\pi} Q \frac{\lambda_c^3}{n^3 V} \quad (2)$$

where  $n$  is the refractive index of GaAs, and  $V$  is the modal volume, which may be calculated using guided-mode expansion method calculations to be  $V = 0.02\lambda_c^3$ . One may therefore estimate that the Purcell factor of a QD on resonance with the mode may be as large as  $F_p = 370$ . To examine therefore whether emission will still couple significantly to the mode even for the largest detuning measured of  $\lambda_c - \lambda_{QD} = 16 \Delta\lambda$ , we make the assumption that the QD is ideally spatially positioned, and rewrite Eq. (1) as  $(\tau/\tau_0) = 2/3 \cdot 370 \cdot 10^{-3} + \alpha = 0.25 + \alpha$ . The Purcell enhancement at this wavelength would therefore be 0.25 times that in free space.

The criterion for strongly polarized emission however, is the ratio of emission rate into the mode relative to the total emission rate, including into leaky modes,  $\beta = 0.25/(0.25 + \alpha)$ . Emission into the mode will be polarized, whereas emission into the leaky modes is unlikely to be polarized: the value of  $\alpha$  is therefore the critical factor governing the mode emission in our case. It was recently reported that, unlike in most micropillar structures, emission into leaky modes may be highly suppressed in the in-plane direction of photonic crystals, such that the spontaneous emission rate in the 2D photonic crystal is reduced with respect to free space by an order of magnitude [11]. Thus, with an estimated value of  $\alpha = 0.1$ , a value of  $\beta = 0.71$  is obtained, and we see that even at strong detuning, emission into the mode may dominate over emission into the leaky modes, and thus strongly polarized emission may be observed.

One would perhaps expect to observe a strong dependence of polarization on the detuning of the QD relative to the mode. In our case, no discernable variation of QD polarization is observed as a function of detuning, either for QDs in the region of Mode 1 (Fig 4) or Mode 3 (Fig 3): however, we did not investigate QDs detuned from this resonance even further, as the QD signal becomes increasingly weak. We also note that strong polarization was observed for all QDs in the mode region: this would imply that either all the QDs are close to ideally placed inside the cavity, or that QDs in non-optimum positions are too weak to be observed, due to the lack of relaxation channels into leaky modes.

An alternative explanation is that only emission into the cavity mode is detected even at large detunings, since emission into leaky modes may not be coupled efficiently to the detection optics as the cavity modes (although the results of [11] indicate that the leaky modes should in fact couple strongly to the out-of-plane direction). The numerical aperture of the objective used is  $\sim 0.42$ , such that modes with stronger vertical emission would be collected more efficiently. This experimental artefact may enhance the polarization of the collected

emission, but would not, by itself, explain our results. If the QD were decoupled from the mode and were to emit into leaky modes only, no emission polarization would be detected.

While the exact mechanism responsible for coupling the QD to the mode is not understood, these results imply that the mode has a significant influence on the QD emission, even when far from resonance. These results are in line with results in ref [8,10], which show that in a system where strong coupling was observed on-resonance, the mode and QD are correlated on the single-quanta level, despite being strongly detuned. Our results suggest, therefore, that the mode and QD are coupled when strongly detuned, even in a system where strong coupling is not possible. While it has been commented [8,10] that this coupling indicates a deviation from the two-level artificial atom model, we demonstrate here that, due to suppression of emission into leaky modes and possible large Purcell factors, one cannot rule out a simple two-level model to explain these results.

#### **4. Conclusions**

In conclusion, we have used mode-resonant enhanced excitation for cavity localised excitation of individual QDs inside a photonic crystal nanocavity. By resonantly exciting into higher-order photonic modes, carriers are absorbed in QDs in the cavity region only. The technique results in efficient excitation of the QDs, and suppression of background PL from the surrounding 2D PhC lattice. We measured the linear polarization of the individual QDs as a function of spectral detuning from higher-order and fundamental modes, and found that the QD lines show the same very strong linear polarization as the modes themselves. This effect persists even when the QD and the mode are spectrally detuned by as much as 16 mode linewidths. While at present we are unable to verify that one mechanism only dominates in our system, it is clear that some process exists that allows coupling between the QD and mode, even when spectrally detuned by up to 16 modal linewidths. Careful consideration of the behavior of a two-level system in a PhC environment shows that coupling to the mode may dominate the emission characteristics to far greater extent than one might at first suppose. These results indicate that it may be possible to couple of two spectrally distinct QDs via a cavity mode even in the weak coupling regime, and they also demonstrate that off-resonant QDs may affect the fidelity of single photon emitters.